[Article ID] 1003- 6326(2002)04- 0712- 04

Crystal structure and thermal stability of martensite in Cu-25Al-3Mn alloy①

LI Zhou(李 周)[1, 2], WANG Ming-pu(汪明朴)[1], CAO Ling-fei(曹玲飞)[1],
XU Gen-ying(徐根应)[2], SU Yu-chang(苏玉长)[1]
(1. Department of Materials Science and Engineering, Central South University, Changsha 410083, China;
2. School of Materials Science and Engineering, Hefei University of Technology, Hefei 230009, China)

[Abstract] The martensite structure in Cu-25Al-3Mn alloy and its thermal cycling and aging behavior are studied. It is convinced that the M2H martensite can be obtained by water-quenched, and the atoms distribution on the basal plane of the martensite is: Ⅰ(corner) —Al; Ⅱ(center of the plane) —Cu; Ⅲ(middle of *b*-side) —22/25Cu+ 3/25Mn. The lattice parameters are determined to be a= 0.445 9 nm, b= 0.527 9 nm, c= 0.424 1 nm, β= 88.64°. The triangle and other complicated configurations consisting of the variant group in the martensite are discovered. It is showed that the tested alloy has a high thermal stability when aging at average temperature in the parent phase, and the thermoelastic martensite amount is up to 90% after aging for 96 h at 400 ℃. The thermal cycling has a little influence on the transformation temperature (M_s). When the number of thermal cycles is up to 1000, the increasing of M_s is only 8 ℃.

[Key words] shape memory alloy; Cu-Al-Mn alloy; thermal stability; thermal cycling
[CLC number] TG 146 [Document code] A

1 INTRODUCTION

Cu-based shape memory alloys (SMAs) have potential application because of their low cost, relatively simple processing and good shape memory effect. The studies on Cu-based shape memory alloy mainly focuses on Cu-Zn-Al alloy and Cu-Al-Ni alloy. The shape memory effect in these alloys is associated with thermoelastic martensite transformation. Many papers reported that the martensite structures in Cu-Zn-Al and Cu-Al-Ni alloys possess 9R (or 18R), 3R(or 6R) and 2H structure depending on the alloy composition, heat treatment and the stress-induced condition[1~4]. In recent years, lots of researchers pay close attention to the study of Cu-Al-Mn alloy because it has many advantages such as the higher shape memory strain, the larger recovery power and better ductility[5~9]. In this paper, the structure of the martensite in the Cu-25Al-3Mn (mole fraction, %) alloy is studied and the thermal stability of the martensite during aging and thermal cycling is studied as well.

2 EXPERIMENTAL

The tested alloy Cu-25Al-3Mn (mole fraction, %) was induction melted, cast into flat ingots, homogenized at 1 123 K for 24 h, then hot-rolled into sheets of 1 mm thick after the surface defects of the ingots were cut off. The sheets were solution-treated at 1 073 K for 10 min and then water-quenched. The tested alloy was confirmed to have ordered phase of DO_3 by X-ray diffractometry. The transformation temperatures were: M_s= 343 K, M_f= 313 K, A_s= 378 K, A_f= 401 K. The specimen was mechanically polished to 0.15 mm, and then jet electro-polished in a solution of 67% CH_3OH+ 33% HNO_3(volume fraction) at about 253 K. The electron microscope used was H-800 operated at 200 kV. X-ray diffraction experiment and data processing were performed on a D-5000 diffractometer with powder specimens whose particle size is less than 75 μm. The powder specimens were solution-treated at 1 073 K for 10 min in a sealed quartz tube filled with argon, followed by water quenching.

3 RESULTS AND DISCUSSION

3.1 Structure of martensite

Fig. 1(a) shows the optical micrograph of the martensite. Besides three variants of AC, AD, AB, a triangle configuration($1^{\rightarrow}$, $2^{\rightarrow}$) and other complicated ones can be observed. This kind of complicated configuration in the Cu-based alloy does not be reported until now. Its crystallographic structure and the effect of it on the shape memory effect are not clear.

Fig. 2(a) is the TEM BF image of the martensite in the tested alloy. The upper variants in the field display an obvious twin sub-structure feature. Fig. 2 (b) shows the diffraction pattern taken from the upper variant, which is a twin-related pattern. The

① [Foundation item] Project (50071069) supported by the National Natural Science Foundation of China
[Received date] 2001- 10- 08

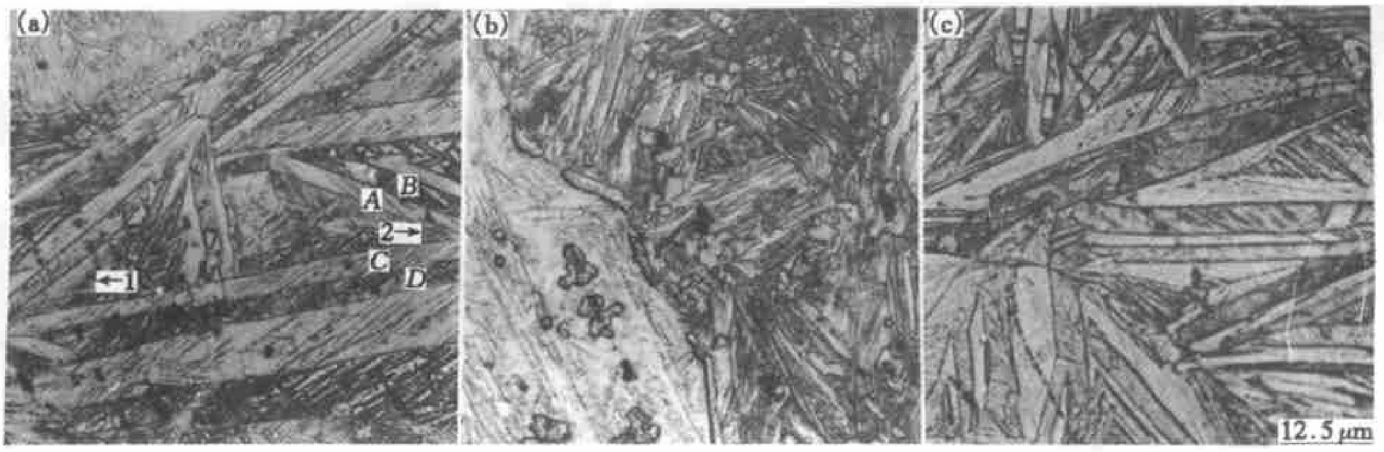

Fig. 1 Optical micrograph of Cu-25Al-3Mn alloy
(a) —Quenching state; (b) —Aging at 400 ℃ for 96 h; (c) —Aging at 350 ℃ for 8 h

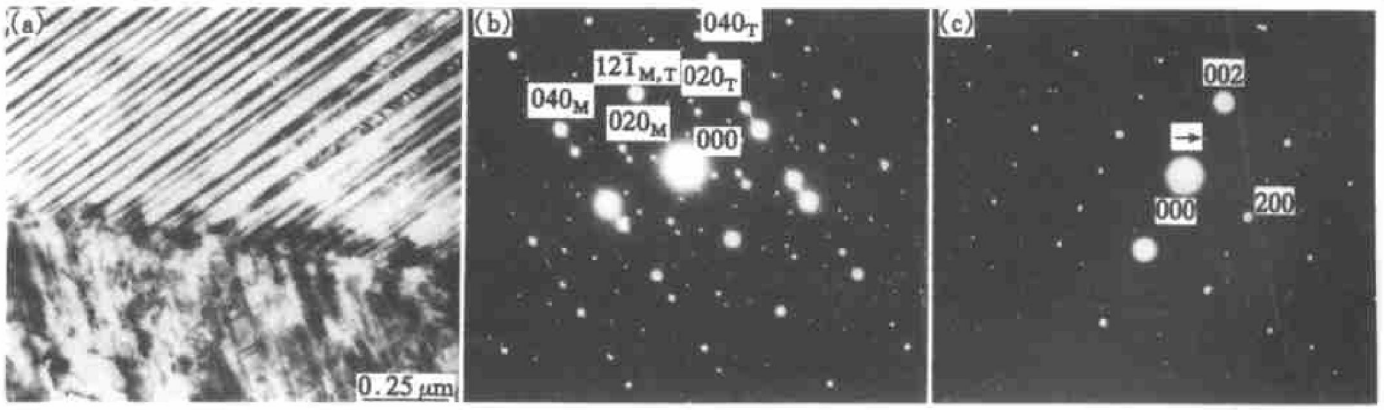

Fig. 2 TEM BF image(a), electron diffraction pattern of $[\bar{1}0\bar{1}]_M$ zone (b) and electron diffraction pattern corresponding to $[0\bar{1}0]_{2H}$ zone (c) of martensite tested

diffraction spots of matrix and twin can be indexed. Fig. 2(c) shows the electron diffraction pattern taken from other field. An weak diffraction spot in the reciprocal unit interlayer spacing (RUIS) along the c^* axis divides the RUIS into two equal parts, and this is the typical feature of 2H structure. The diffraction pattern corresponds to the $[0\bar{1}0]_{2H}$ zone of the martensite. Because the diffraction spots of (002) and (200) simultaneously appear in this diffraction pattern, the angle (β^*) between a^* axis and c^* axis can be measured and determined to be 91.4°(and so, the angle β between a axis and c axis is 88.6°). Therefore, this 2H structure is monoclinic one (M2H).

Fig. 3 shows the X-ray diffraction pattern of the martensite in the tested alloy. All of the diffraction peaks can be indexed in accordance with 2H structure. The measured d values (d_m) of each diffraction peak and its relative integrated intensities measured are shown in Table 1. The lattice parameters, a= 0.445 9 nm, b= 0.527 9 nm, c= 0.424 1 nm, β= 88.64°, can be determined from the d_m values.

Fig. 4 shows the hard sphere atomic structure model of the M2H martensite. There are only 4 kinds of different positions, i.e., I, II_1, II_2, III, on the

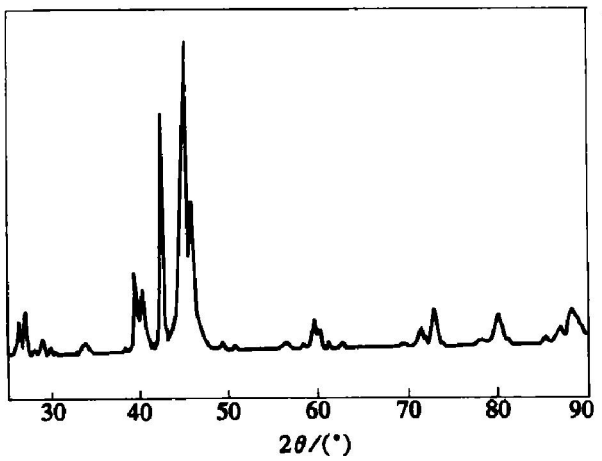

Fig. 3 X-ray diffraction spectrum of water-quenched martensite of Cu-25Al-3Mn alloy

basic plane (as shown in Fig. 4(a)). No matter how many sorts and much amounts of atom are distributed, its structure factor can be expressed as:

$$F_{HKL} = [f_{\mathrm{I}} + f_{\mathrm{III}}\exp 2\pi i(K/2) + f_{\mathrm{II}_1}\exp 2\pi i \cdot (H/2 + K/4) + f_{\mathrm{II}_2}\exp 2\pi i(H/2 + 3K/4)] \cdot [1 + \exp 2\pi i(HM + K/2 + L/2)] \quad (1)$$

where M is the coordinate of the first layer along the a axis.

Table 1 Data of X-ray diffraction measurement and calculation of water-quenched Cu-25Al-3Mn alloy

Peck No.	*HKL*	d_m/nm	d_c/nm	$(I/I_{12\bar{1}})_m \times 10^{-2}$	$(I/I_{12\bar{1}})_c \times 10^{-2}$
1	110	0.340 2	0.340 6	10.9	11.3
2	011	0.330 7	0.330 6	12.8	13.3
3	101	0.307 3	0.307 3	4.0	4.6
4	020	0.264 5	0.264 0	6.8	7.5
5	120	0.227 0	0.227 1	40.5	41.9
6	200	0.223 0	0.223 0	28.4	29.0
7	002	0.212 0	0.212 0	75.8	75.9
8	$12\bar{1}$	0.200 4	0.200 2	100.0	100.0
9	201	0.197 4	0.197 4	41.9	41.4
10	122	0.155 0	0.155 0	13.5	11.0
11	$12\bar{2}$	0.153 6	0.154 0	5.2	5.6
12	040	0.132 0	0.132 0	15.3	13.9
13	320	0.129 6	0.129 5	23.7	25.7
14	$12\bar{3}$	0.120 0	0.120 0	16.4	15.6
15	$32\bar{2}$	0.110 4	0.110 5	14.9	15.4

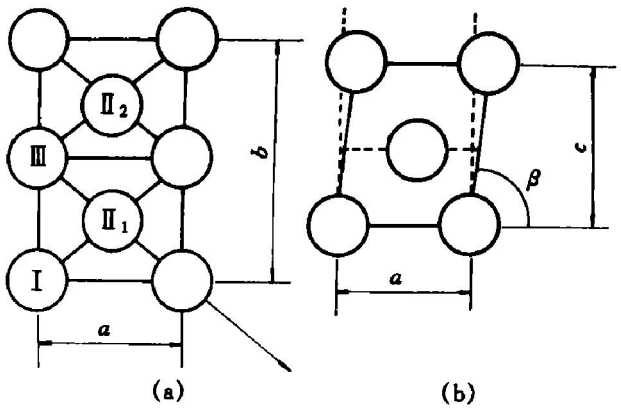

Fig. 4 Crystal structure model of M2H martensite

In Eqn. (1) the first item is the structure factor of the basic plane called as F_a.

Making $F_a = 0$, then the forbidden diffraction can be obtained:

$$K = \text{even},\ H + K/2 = \text{odd or } K = \text{odd} \quad (2)$$

If the atom distribution on the basic plane is in order, the diffraction expressed in Eqn. (2) may occur:

When K = even, $H + K/2$ = odd,

$$F_a = (f_{\text{Ⅰ}} - f_{\text{Ⅱ}}) + (f_{\text{Ⅲ}} - f_{\text{Ⅱ}}) \quad (3)$$

When K = odd, $F_a = (f_{\text{Ⅰ}} - f_{\text{Ⅲ}})$ (4)

According to the experimental parameters, Eqn. (3) represents the atomic ordering state of the nearest neighboring (NN), and Eqn. (4) represents the atomic ordering state of the next nearest neighboring (NNN).

With the hard sphere atomic structure model of the M2H martensite and the hypothesis: 1) the atoms in the basal plane contacts with each other along [210] direction; 2) the layer interval is $c/2$; 3) each atom in the second later contacts with the atoms in Ⅰ, Ⅱ_1, Ⅲ positions in the basal plane, the following equations can be obtained:

$$\begin{cases} [2(r_{\text{Ⅰ}} + 2r_{\text{Ⅲ}} + r_{\text{Ⅱ}_1})]^2 = a^2 + (b/2)^2 \\ (a/2 - x)^2 + (b/4)^2 + (c/2)^2 = \\ \quad (r_{\text{Ⅰ}} + 2r_{\text{Ⅲ}} + r_{\text{Ⅱ}_1})^2 \end{cases} \quad (5)$$

Using the lattice parameters, x (x is the stacking position of the first layer along the a axis) and M can be obtained (x = 0.154 1 nm, M = 1/2.894).

With the structure model above and the composition of the alloy, the diffraction intensity of different ordering state can be calculated. Thinking of the difference of the scattering factor between every two kinds of the atoms of the three elements Cu, Al and Mn and the X-ray diffraction data, the rational atom distribution in basal plane is that the atom on position Ⅰ is Al, Ⅱ is Cu, Ⅲ is 3/25Mn + 22/25Cu.

Then the structure factor of the basic plane can be expressed as follows.

For the fundamental diffraction:

$$F_a = 72/25 f_{\text{Cu}} + 25/25 f_{\text{Al}} + 3/25 f_{\text{Mn}}$$

For the NN order diffraction:

$$F_a = 25/25 f_{\text{Al}} + 3/25 f_{\text{Mn}} - 28/25 f_{\text{Cu}}$$

For the NNN order diffraction,

$$F_a = 25/25 f_{\text{Al}} - 22/25 f_{\text{Cu}} - 3/25 f_{\text{Mn}} \quad (6)$$

Considering the Lorent-polarization and multiplicity factors, the relative integrated intensities of the diffraction peaks concerned can be calculated (as shown in Table 1). It can been seen that the I_c coin-

cide satisfactorily with the I_m.

3.2 Thermal stability of martensite during aging and thermal cycling

Fig. 5 shows the relation of the thermoelastic martensite amount and the aging time at 400 ℃. Although the aging time is up to 96 h, the thermoelastic martensite amount keeps 90% yet. This amount is much higher than that of the Cu-Zn-Al alloy and the Cu-Al-Ni-Mn-Ti alloy[10, 11]. Fig. 1(b) shows optical micrograph of the tested alloy aged at 400 ℃ for 96 h. From the image, only precipitation of γ_2 phase can be seen. For the Cu-Zn-Al and Cu-Al-Ni-Mn-Ti alloys, when they were aged at average temperature for a relatively long time (3~8 h)[10, 11], the β_1 phase transforms into bainite or decomposes into equilibrium phase, and the thermoelastic martensite amount decreases rapidly.

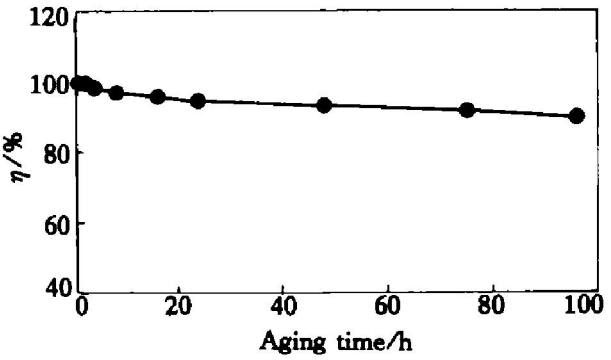

Fig. 5 Relation of thermoelastic martensite amount and aging time at 400 ℃

Fig. 6 shows the effect of the number of thermal cycling on the transformation temperature (M_s). The thermal cycling is carried out at the temperature ranging from 20 ℃ to 350 ℃. It has been found that the thermal cycling has a little influence on the transformation temperature of the tested alloy. When the cycles are up to 1 000, the increasing of M_s is only 8 ℃. Several mechanisms have been proposed for the change of transformation temperature induced by thermal cycles. It has been proved that thermal cycling results in the formation of defects such as dislocation in SMA and the presence of the dislocation is favorable to nucleation of martensite, which causes increasing of the M_s temperature[12]. Furthermore, precipitation of secondary phase can cause a chemical composition change in the matrix, and this may induce the change of M_s[13]. The secondary phases do not precipitate while aging at 350 ℃ (as shown in Fig. 1(c)). This factor for the increasing of M_s does not exist in the tested alloy. The increasing of transformation temperature may associate with the first mechanism. It is very important that SMAs maintain a steady transformation temperature during cycling and keep a high thermal stability during aging for the purpose of practical application.

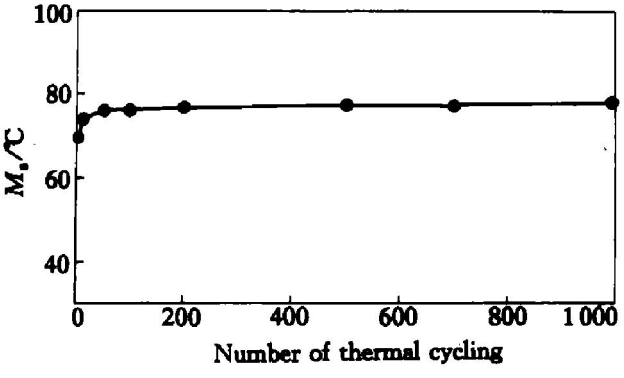

Fig. 6 Effect of number of thermal cycling on transformation temperature

[REFERENCES]

[1] Saburi T, Wayman C M. Crystallographic similarities in shape memory martensite [J]. Acta Metall, 1979, 27: 979-995.

[2] Tadaki T, Tokoro M, Shimizu K. Thermoelastic nature and crystal structure of the Cu-Zn martensite related to the shape memory alloy [J]. Trans JIM, 1975, 16: 285-296.

[3] Tadaki T, Okazaki H, Nakata Y, et al. Atomic configuration studied by ALCHEMI and X-ray diffraction of a stabilized M18R martensite in α β phase Cu-Zn-Al alloy [J]. Mater Trans JIM, 1990, 31: 941-947.

[4] Adachi Kenji, Perkins Jeff. Lattice image studies on the intervariant boundary structure and substructure of Cu-Zn-Al 18R martensite [J]. Met Trans A, 1985, 16A: 1551-1566.

[5] Zak G, Kneissl A C, Zatulskij G. Shape memory effect in cryogenic Cu-Al-Mn alloys [J]. Scripta, 1996, 34 (3): 363-367.

[6] Kainuma R, Takahashi S, Ishida K, Metall thermoelastic martensite and shape memory effect in ductile Cu-Al-Mn alloys [J]. Mater Trans A, 1996, 27A: 2187-2195.

[7] Kainuma R, Takahashi S, Suto Y. Development of a new type of Cu-base shape memory alloys with enhanced ductility [A]. C-J SMA'97 [C]. Hangzhou, 1997. 177-180.

[8] Bubley I R, Koval Yu N, Titov P V. $\beta_1 \rightarrow \gamma'$ Transformation in Cu-Mn-Al alloys after low temperature ageing [J]. Scripta Mater, 1999, 41(6): 637-641.

[9] LI Zhou, WANG Ming-pu, CAO Ling-fei. Crystal structure and thermal stability of martensite in Cu-24Al-3Mn alloy [J]. Trans Nonferrous Met Soc China, 2002, 12(1): 6-10.

[10] WANG Ming-pu, WANG Shi-wei, JIN Zhan-peng. Relief phenomenon of stabilized martensites in a Cu-Zn-Al alloy [J]. J Cent South Univ Technol, (in Chinese), 1997, 28(1): 53-56.

[11] WANG Ming-pu, JIN Zhan-peng, YIN Zhi-min, et al. Effect of non-isothermal β_1-phase aging on thermoelastic martensite transformation of CuAlNiMnTi alloy [J]. Trans Nonferrous Met Soc China, 1996, 6(2): 73-77.

[12] Perkins J, Muesing W E. Martensitic transformation cycling effects in Cu-Zn-Al shape memory alloys [J]. Metal Trans, 1983, 14A: 33-36.

[13] Kennon N F, Dunne D P, Middleton L. Aging effects in copper-based shape memory alloys [J]. Metal Trans, 1982, 13A: 551-555.

(Edited by YANG Bing)